

## Efficiency and Stiffness of the Single Lap Bolt Joints in Glass Epoxy Composites

Jaspreet Singh, Kulwinder Singh, and J.S. Saini\*

Mechanical Engineering Department, Thapar Institute of Engineering and Technology, Patiala - 147 004, India

\*E-mail: jsaini@thapar.edu

### ABSTRACT

The present work deals with the investigations on the joint efficiency and the joint stiffness of the single lap bolt joint made of two dimensional woven glass fibre reinforced composite materials. The effect of joint geometry, bolt pretension and washer has been determined on the bolt joint performance. To estimate the effect of geometric parameters; the edge-to-hole diameter ( $e/d$ ) and width-to-hole diameter ( $w/d$ ) ratios are varied from 3 to 4 and 3 to 5, respectively. To study the worst loading conditions; the bolt pre-tension is set to zero, whereas 5 Nm torque is applied to investigate the joint in fully clamped conditions. Two different sizes of washer *i.e.*, the outer diameter of 12 mm and 16 mm have been studied to estimate the effect of the washer on failure load, joint stiffness, and joint efficiency. Progressive damage analysis has been performed on the single lap bolt joint. Characteristic curve method along with Tsai-Wu failure criteria has been used for the prediction of the failure loads and failure modes. The joint stiffness and the failure load of the joint are increased with the increase of  $w/d$  ratios. However, the joint efficiency was negatively influenced by  $w/d$  ratio.

**Keywords:** Glass fibre; Bolt joint; Joint efficiency; Characteristic curve; Tsai-Wu failure theory

### 1. INTRODUCTION

The efficiency of the machines has become an essential point for competition among automotive and aircraft industries. To reduce the fuel consumption and increase the efficiency; the industry has a considerable focus on the development of lightweight materials giving comparable performance to the traditional metals. Fibre reinforced plastics while being light in weight and having high load bearing capacities are often used in place of traditional sheet metal components in an automobile.

To build any structure and to perform the desired function, different components need to be joined together. The most popular type of joints in the composite applications are the mechanical and the adhesive joints. Compared to the adhesive joint, the mechanical joints incur low cost and facilitate easy disassembly for the maintenance without damaging the primary components.

Different researchers have successfully investigated the effect of important parameters *i.e.*, bolt torque, washer effect, and geometry of a bolt joint on the performance of joint.

McCarthy<sup>1</sup>, *et al.* investigated the effect of bolt hole clearance on strength and stiffness of single bolt; single-lap bolted joint numerically and experimentally. Kweon<sup>2</sup>, *et al.* presented a numerical method to determine characteristic lengths for the prediction of failure modes on a characteristic curve around the hole of the composite joint without any experimentation. Xiao and Ishikawa<sup>3</sup> measured the bearing

damage behaviour of composite bolted joints using acoustic emission technique. Xiao and Ishikawa<sup>4</sup> developed the analytical model to simulate the bearing strength and failure behaviour of laminated composite bolted joint. Kelly<sup>5</sup> investigated the fatigue life, and strength of hybrid (bolted/bonded) carbon fibre reinforced composite single lap joint using two different types of adhesives. Khashaba<sup>6</sup>, *et al.* investigated the effect of bolt preload and washer outer diameter on the strength of glass fibre reinforced epoxy composites with the stacking sequence of  $[0^\circ/\pm 45^\circ/90^\circ]$ . Nassar<sup>7</sup>, *et al.* investigated the behaviour of single lap double bolt in serial composite joint experimentally. Sen<sup>8</sup>, *et al.* determined the bearing strength, and failure modes of bolted joint under preload and with different geometrical parameters. Asi<sup>9</sup>, *et al.* determined the effect of linear density of woven glass fibre on the bearing strength of glass fibre reinforced epoxy laminated composite mechanical joint. Egan<sup>10</sup>, *et al.* studied the bolt hole clearance effects in single lap, single bolt countersunk composite joint using nonlinear elements in ABAQUS code. Irisarri<sup>11</sup>, *et al.* developed a refined finite element model for the prediction of the bearing strength of single fastener joint in carbon fibre reinforced plastic composites. Qin<sup>12</sup>, *et al.* determined the effect of protruding head and countersunk fastener on the mechanical behaviour of double lap composite bolted joint. Gray<sup>13</sup>, *et al.* performed experiments on countersunk multi-bolt joints to estimate their stiffness and strength with respect to tapering, and thickness of laminates. Zhai<sup>14</sup>, *et al.* investigated the bearing strength, and joint efficiency of single lap, single bolt countersunk

joint. Sekhon<sup>15</sup>, *et al.* studied the influence of geometric parameters *i.e.*, edge-to-hole distance ( $e/d$ ) and width-to-hole distance ( $w/d$ ) experimentally and numerically. Singh<sup>16</sup>, *et al.* studied the effect of nanoclay on failure mode and strength of unidirectional glass fibre reinforced epoxy composite pin joint. Mara<sup>17</sup>, *et al.* investigated the effect of metallic insert in drilled hole, on the stiffness and bearing behaviour of joints. Singh<sup>18</sup>, *et al.* studied the effect of metal inserts on the strength of pinned joints in glass fibre reinforced composites.

It is observed from the literature review that there are some parameters such as joint geometry, materials used, stacking sequence, joint configuration, fastening parameters, and the type of loading, which affects the ultimate failure load and failure mode of the composite laminate joints. Apart from these parameters, bolt pretension and washer size can also be very influential on the joint efficiency and failure mechanism. The effect of these two parameters is not much studied in the literature. Hence, the present work deals with the investigation of the effect of joint geometry, bolt pretension and washer size on the joint performance.

## 2. EXPERIMENTATION

The following section details about the materials, preparation of laminated polymer composite and performance analysis of the bolt joint made of glass fibre reinforced composite.

### 2.1 Materials

#### 2.1.1 Glass Fibre

Two-dimensional woven 'Advantex' glass fibre with 360 gsm, supplied by Owens Corning India Pvt. Ltd., Mumbai, India, was used in the present work. The tensile strength and young modulus in tension for the fibre are 3100 g/mm<sup>2</sup> - 3800 g/mm<sup>2</sup> and 80 GPa - 81 GPa, respectively.

#### 2.1.2 Resin

The diglycidyl ether of bisphenol A (DGEBA) based epoxy resin (L-12), hardener (K-12) and accelerator (K-13) were used to prepare the matrix. The chemical structure of the DGEBA based epoxy is as given in Fig. 1. The chemical name of Hardener (K-12) is anhydride and that of accelerator (K-13) is triamine. The resin, hardener, and accelerator were supplied by Atul Ltd., Gujarat, India.

The tensile modulus, tensile strength, flexural strength, and compressive strength of the epoxy-based resin is 15000 N/mm<sup>2</sup> - 16000 N/mm<sup>2</sup>, 70 MPa - 90 MPa, 100 MPa - 120 MPa, and 190 MPa - 210 MPa. These properties are as per the data sheet provided by the supplier.

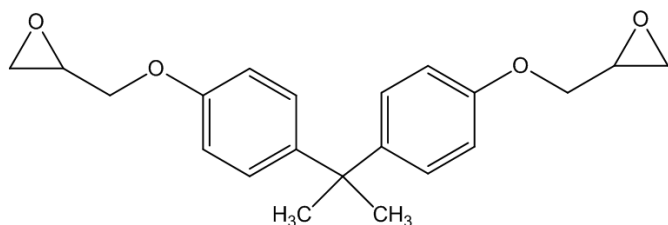


Figure 1. Chemical structure of the DGEBA based epoxy.

### 2.2 Composite Preparation

The glass fibre laminas were cut to adequate size. The epoxy resin and hardener were mixed together in the mechanical stirrer at 8000 rpm for 15 min as per the instructions provided by the supplier. After the proper mixing of the epoxy resin and the hardener, the accelerator is added to the mixture. The hand-layup technique was used to prepare the laminate of desired thickness. After that, laminates were cured at room temperature for 40 h - 50 h followed by curing in the compression molding machine at optimised<sup>19</sup> curing parameters *i.e.*, the temperature of 150 °C, the pressure of 140 kN, and hold time of 30 min.

#### 2.2.1 Material Characterisation

The tensile, shear, and compressive strength of the composite laminate were evaluated as per ASTM D3039<sup>20</sup>, D695<sup>21</sup> and D5379<sup>22</sup>, respectively. Figure 2 shows the specimen configurations for tensile, compression and shear testing of the laminates. Five specimens each were tested on German make Zwick-Roell Universal Testing Machine for tensile, compression and shear tests at the cross-head speed of 2 mm/min, 1.3 mm/min and 2 mm/min, respectively. The maximum percentage error in the full factorial experiment was < 5 %. The standard deviations were in the range of 10-12 %.

The mechanical properties of the prepared composite laminate are as shown in Table 1. The bidirectional woven glass fabric along with the alternate and symmetrical stacking sequence was used to manufacture the composite laminates in the present work. The use of bidirectional woven glass fabric and the alternate and symmetrical stacking sequence balanced the properties in both the longitudinal and transverse directions. The laminates were tested for tensile strength in both the directions which came to be the same. So the other properties were tested in one direction only and were assumed to be identical in the other direction as the fabric is bidirectional woven with alternate and symmetric stacking sequence.

Table 1. Mechanical properties of laminate

Mechanical property	Symbol	Magnitude
Longitudinal strength in tension	$X_t$	428 MPa
Transverse strength in tension	$Y_t$	428 MPa
Longitudinal strength in compression	$X_c$	270 MPa
Transverse strength in compression	$Y_c$	270 MPa
Shear strength	$S_{12}$	104 MPa
Longitudinal modulus	$E_{11}$	21.68 GPa
Transverse modulus	$E_{22}$	21.68 GPa
Poisson ratio	$\nu_{12}$	0.148

### 2.3 Preparation of Bolt Joint

The geometry of the single lap bolt joint specimen is as shown in Fig. 3, where,  $d$  is the diameter of the hole,  $e$  is the hole to edge distance,  $w$  is the width,  $t$  is the thickness of the specimen and  $D$  is the outer diameter of the washer.

The different geometric configurations and torque settings used to analyse the performance of the bolt joint are as shown in Table 2. To estimate the effect of the washer; on failure load, joint stiffness and joint efficiency, two different sizes of washer *i.e.*, the outer diameter of 12 mm and 16 mm have been studied. To study the worst loading conditions; the bolt pre-tension is set

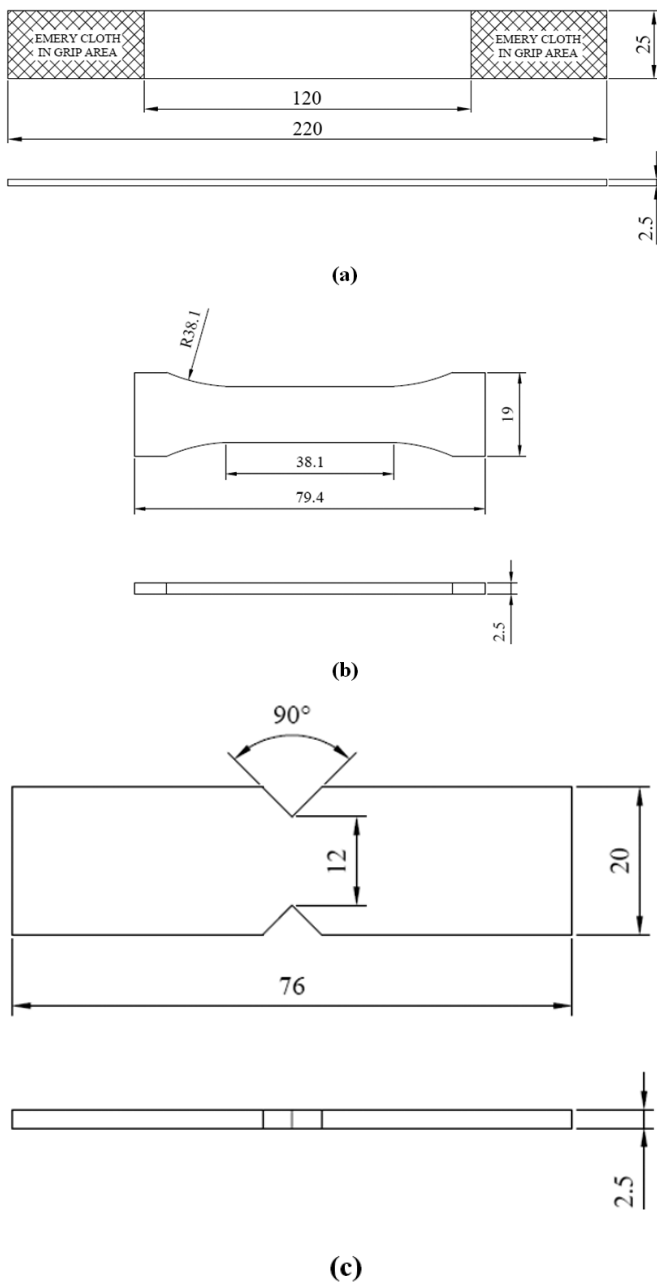


Figure 2. Specimen configuration for the (a) Tensile test, (b) Compression test, and (c) Shear test.

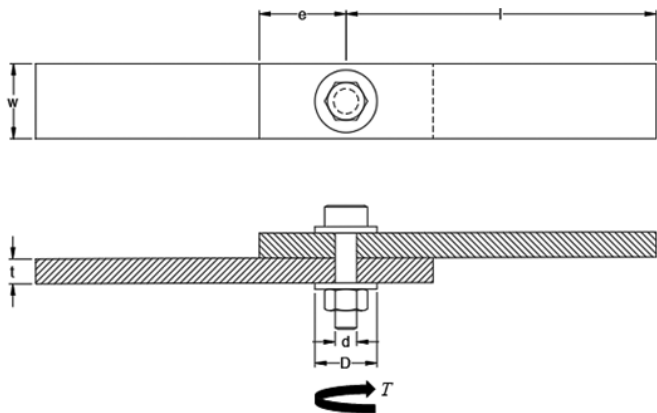


Figure 3. Geometric parameters of single lap single bolt joint.

Table 2. Different configurations of joint with a hole diameter ( $d$ ) of 6 mm and specimen thickness ( $t$ ) of 2.5 mm

Specimens	$w/d$ ratio	$e/d$ ratio	$w$ (mm)	$e$ (mm)	Torque (Nm)	Washer outer diameter (mm)
1	3	3	18	18	0	Without
2	3	3	18	18	0	12
3	3	3	18	18	0	16
4	3	3	18	18	5	12
5	3	3	18	18	5	16
6	4	3	24	18	0	Without
7	4	3	24	18	0	12
8	4	3	24	18	0	16
9	4	3	24	18	5	12
10	4	3	24	18	5	16
11	5	3	30	18	0	Without
12	5	3	30	18	0	12
13	5	3	30	18	0	16
14	5	3	30	18	5	12
15	5	3	30	18	5	16
16	3	4	18	24	0	Without
17	3	4	18	24	0	12
18	3	4	18	24	0	16
19	3	4	18	24	5	12
20	3	4	18	24	5	16
21	4	4	24	24	0	Without
22	4	4	24	24	0	12
23	4	4	24	24	0	16
24	4	4	24	24	5	12
25	4	4	24	24	5	16
26	5	4	24	30	0	Without
27	5	4	24	30	0	12
28	5	4	24	30	0	16
29	5	4	24	30	5	12
30	5	4	24	30	5	16

to zero, whereas 5 Nm torque is applied to investigate the joint in fully clamped conditions. To estimate the effect of geometric parameters; the  $e/d$  and  $w/d$  ratios are varied from 3 to 4 and 3 to 5, respectively. Bolt joint without washer and bolt pre-tension behaves as a pin joint configuration, this configuration was used to compare its joint efficiency with that of bolt joint configuration. The high tensile bolts with a shank diameter of 6 mm and the washer with the inner diameter of 6.02 mm were used for the investigation.

### 3. RESULTS AND DISCUSSION

Bolt joints were tested under tensile load on Zwick-Roell Universal Testing Machine as per ASTM D3039 at a crosshead speed of 2 mm/min. The load-displacement curves generated through the testing of the single lap, single bolt joint under different configurations are as shown in Fig. 4.

It is clear from the Fig. 4 that the load-displacement curves are linear in the initial stage. However, after initial failure *i.e.*, the first peak point, the load-displacement curve depicts the non-linear behaviour *i.e.*, the strain is more than the stress. For both preload levels *i.e.*, 0 Nm and 5 Nm, the specimen with  $w/d = 3$  failed in net-tension mode, whereas bearing failure mode for both was observed with  $w/d = 5$ . Unlike the specimens with  $w/d = 3$  and 5, different failure modes were observed at different preloads *i.e.*, 0 and 5 Nm in the specimen having  $w/d = 4$ . Specimen with 0 Nm torque failed in bearing whereas net-tension failure mode was observed for the specimen with 5 Nm

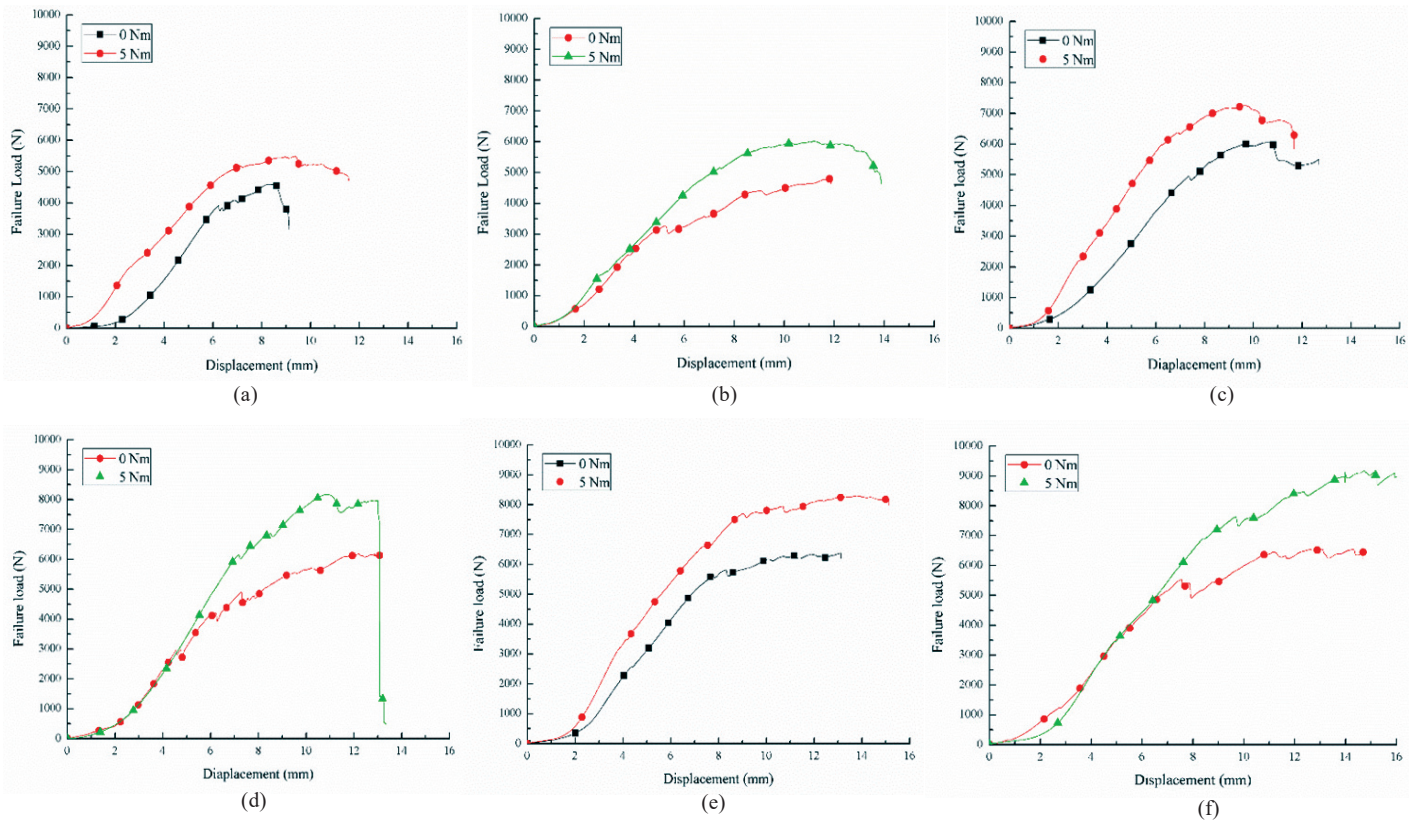


**Figure 4.** Load versus displacement curve for (a)  $w/d = 3$ ,  $e/d = 4$ , Washer 12 mm, (b)  $w/d = 3$ ,  $e/d = 4$ , Washer 16 mm, (c)  $w/d = 4$ ,  $e/d = 4$ , Washer 12 mm, (d)  $w/d = 4$ ,  $e/d = 4$ , Washer 16 mm, (e)  $w/d = 5$ ,  $e/d = 4$  Washer 12 mm, and (f)  $w/d = 5$ ,  $e/d = 4$  Washer 16 mm.

torque, for the said configuration.

Compared to the specimen with  $w/d = 4$ , the specimen with  $w/d = 3$  failed in a sudden manner. Investigating the maximum displacements before catastrophic failure, the specimens with  $w/d = 4$  demonstrated larger displacements compared to the specimen with  $w/d = 3$ , which could be due to higher load-bearing capacity and, consequently larger out of plane displacement of the specimen with  $w/d = 4$  due to eccentricity of load applied. The specimens with  $w/d = 3$  failed directly in net-tension without undergoing out of plane displacement as shown in Figs. 4 (a) and (b). Whereas, a specimen with  $w/d = 4$  showed out of plane displacement prior to the catastrophic failure *i.e.*, net-tension. Increasing  $e/d$  ratio from 3 to 4 for a particular joint configuration, there is no significant effect on the maximum failure load of the joint and due to this the load-displacement curves for  $e/d = 4$  only are presented in this study. Both initial and ultimate failure load increases with an increase in bolt pretension. However, increasing the outer diameter of the washer demonstrated a negative effect on the initial failure load in the identical conditions. Initial failure load decreases with 16 mm washer outer diameter and, damage becomes more progressive which may be the result of the larger confinement area of the washer and the wider area of damage with larger outer diameter washer. A delay in stiffness loss after initial failure of the single lap joint is observed with increase in the  $w/d$  ratio because the reduction in stiffness after the initial failure in the specimen of  $w/d = 5$  was less than that of at  $w/d = 4$ . It is due to the higher resistance offered by the large width

to the secondary bending of the joint due to eccentric loading.

The fibre reinforced composite joints fail in different failure modes such as bearing mode, net-tension mode, shear-out mode or the combination of all these. The actual images of some of the failed specimens during experiments are as displayed in Fig. 5. For  $w/d = 3$ , as shown in Fig. 5(a) and (b), both the specimens at 0 Nm and 5 Nm torque failed with the net-tension failure mode. As the  $w/d$  ratio changes from 3 to 4, in case of finger tight condition, the failure mode changed to bearing from net-tension. However, it remains a net-tension mode for a torque of 5 Nm, as shown in Fig. 5(d). At  $w/d = 5$ , instead of catastrophic failure, progressive failure take place. In case of finger tight conditions at  $w/d = 5$  as shown in Fig. 5(e), although significant delamination is observed near the hole, still the failure mode is bearing. In fully clamped conditions, as shown in Fig. 5(f), lateral constraint provided by washer reduced the delamination and also reduced the degree of damage near the hole. Besides severe damage, at this  $w/d$  ratio, the failure mode was bearing at a torque of 5 Nm, instead of a catastrophic failure *i.e.*, net-tension.

The width of the specimen is an important design parameter as it could affect the load carrying capacity of the joint. The ultimate load carrying capacity of specimen increases with increase in width-to-diameter ( $w/d$ ) ratio and bolt pretension, as shown in Fig. 6. Corresponding to the different failure modes (bearing or net-tension) at different  $w/d$  ratios, failure load is increased when  $w/d$  is changed from  $w/d = 3$  to 4. Increasing the  $w/d$  ratio beyond 4 has no effect on

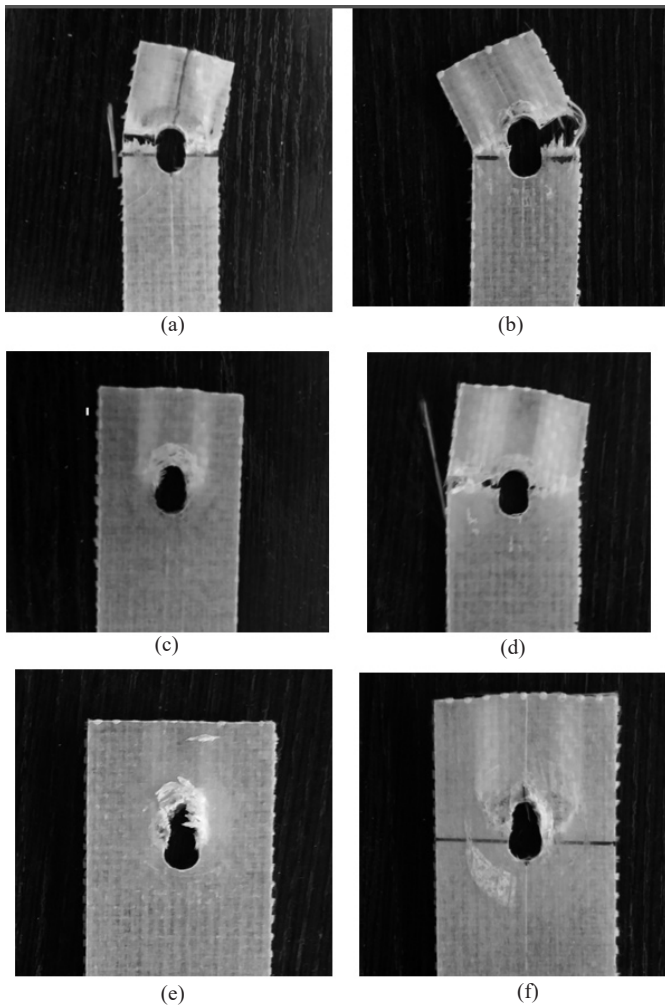


Figure 5. Failure mode at (a)  $w/d = 3$ , Torque = 0 Nm, (b)  $w/d = 3$ , Torque = 5 Nm, (c)  $w/d = 4$ , Torque = 0 Nm, (d)  $w/d = 4$ , Torque = 5 Nm, (e)  $w/d = 5$ , Torque = 0 Nm, and (f)  $w/d = 5$ , Torque = 5 Nm.

the failure load as the failure mode remains bearings at 0 Nm. However, failure load increased when  $w/d$  ratio changes from 4 to 5 at 5 Nm pretention because failure mode also changes from net-tension to bearing at the said torque level.

The effect of torque on failure load was observed at each value of  $w/d$  ratio and each type of washer. For higher  $w/d$  ratio, the effect of torque is more. The effect of  $e/d$  ratio, which is related to the shear failure behaviour of the joint was negligible as no shear failure behaviour was observed in the single lap single bolt joint. The ultimate failure load for different geometric configurations, different torque settings and different type of washers are also shown in Fig. 6. Increasing bolt pre-tension from 0 to 5 Nm, failure load increases by 25 per cent for lower  $w/d$  ratio whereas 42 per cent increase in failure load was observed for higher  $w/d$  ratio. As the washer outer diameter increases, knee growth of damage takes place which is observed in most of the load-displacement curves of specimens tested with the washer of 16 mm outer diameter. This type of damage takes place due to the decrease in pressure with an increase in lateral constraint area. However, the ultimate failure load increases which is due to the increase in the damage distribution area.

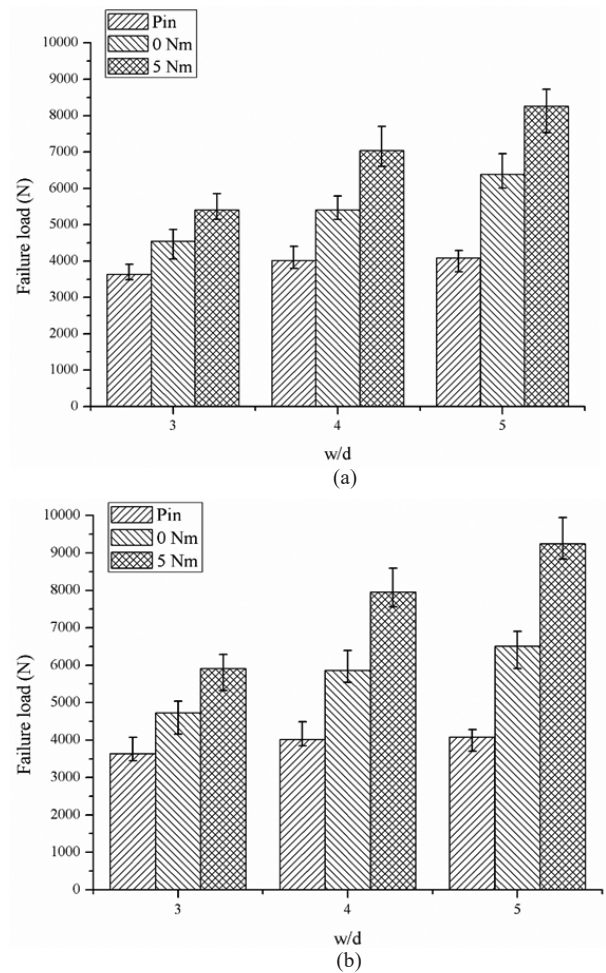


Figure 6. Failure load at  $e/d = 3$  and with washer of size (a) 12 mm and (b) 16 mm.

### 3.1 Joint Efficiency

Joint efficiency is an integral part of the joint analysis. It can help to optimise the different joint parameters. For the specimen with  $e/d = 3$  and different  $w/d$  ratio, tightening conditions, and the outer diameter of the washer, the joint efficiency ( $\eta$ ) as shown in Fig. 7, has been evaluated by using Eqn. (1).

$$\eta = \frac{R_p}{R_s} \tag{1}$$

where  $R_p$  is resistance of plate per pitch length and  $R_s$  is resistance offered by the solid plate.  $R_p$  was measured as the resistance offered by the lap joint whereas  $R_s$  was measured as the resistance offered by the solid specimen (without the hole) of the identical geometric parameters. Both these resistances were taken as forces and were measured experimentally on the universal testing machine to calculate the efficiency of the joint for different joint configurations.

The decrease in efficiency when the  $w/d$  ratio changes from 3 to 4, reveals that the load carrying capacity of the joint does not increase as much as the load carrying capacity of laminate solid plate increases. Maximum efficiency was recorded at  $w/d = 3$  with 5 Nm bolt preload and washer outer diameter 16 mm however, failure was observed catastrophic. In comparison to

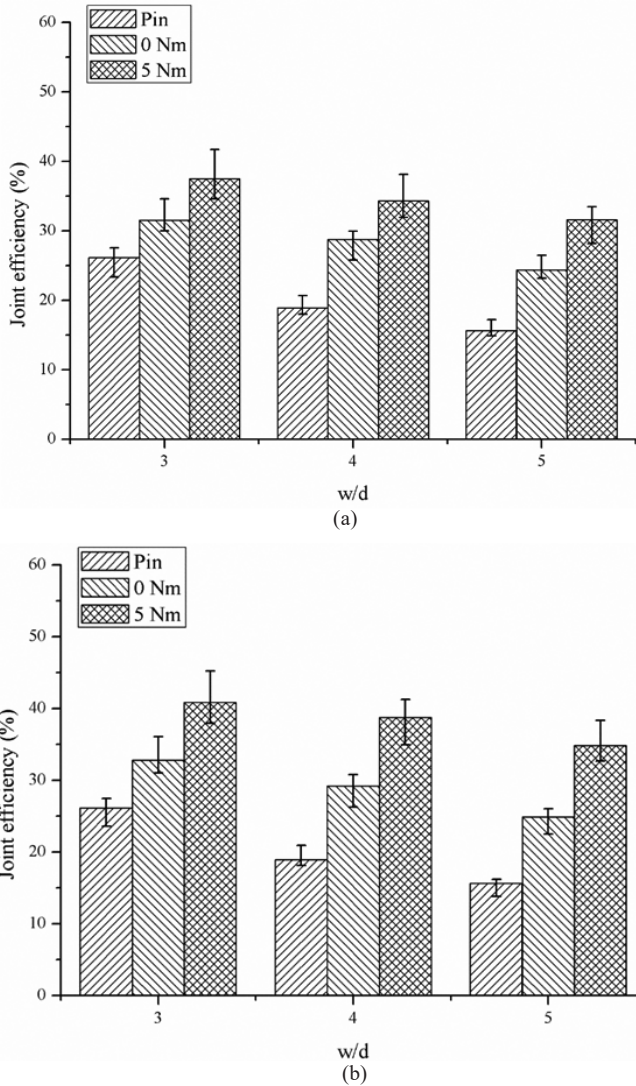


Figure 7. Joint efficiency at  $e/d = 3$  and washer of size (a) 12 mm and (b) 16 mm.

the pin joint, the efficiency of joint with the use of washer at zero Nm torque is increased by 5 per cent. At  $w/d$  ratio as 4 and 5, although the bearing failure mode was observed in most of the cases and the failure load found to be increased, but the joint efficiency remained almost the same. It can be seen that the efficiency is almost constant after  $w/d$  ratio as 4. It can also be seen from the Fig. 7 that the joint efficiency increases with increase in torque.

### 3.2 Joint Stiffness

The joint stiffness and joint strength are the crucial factors of structural design. Figure 8 shows the effect of washer diameter, and torque on the joint stiffness. The two distinct parts of the curves as shown in Fig. 8 gives the variation of the joint stiffness with the variation of the  $w/d$  ratio. The two parts of the curves gives the variation of joint stiffness for  $w/d$  ratio to be 3 to 4 and 4 to 5, respectively.

The outer diameter of the washer and the  $w/d$  ratio have shown significant effects on the joint stiffness. With increase in the  $w/d$  ratio the stiffness increases. Whereas, stiffness reduces by increasing the outer diameter of the washer. As shown in Fig. 8; the slope of the curve or stiffness is higher between  $w/d$  ratio = 4 and 5 than the slope of the curve or stiffness between  $w/d = 3$  and 4. It is due to the reason that with the increase in  $w/d$  ratio, the clamping area increases. However, the active pressure imparted by washer decreases as the outer diameter of washer increases. The reduction in effective pressure reduces the stiffness of the joint.

The pressure applied through washer was calculated using Eqn. (2) given by Park <sup>23</sup>, *et al.*

$$\sigma_{press} = \frac{1000T}{\left(\frac{\pi}{4}\right)kd(D^2 - d^2)} \quad (2)$$

where  $T$  is the applied torque (Nm),  $\sigma_{press}$  is bolt pretension pressure (MPa),  $D$  is washer outer diameter (mm),  $d$  is nominal diameter of bolt (mm) and  $k$  is torque coefficient which was taken as 0.2.

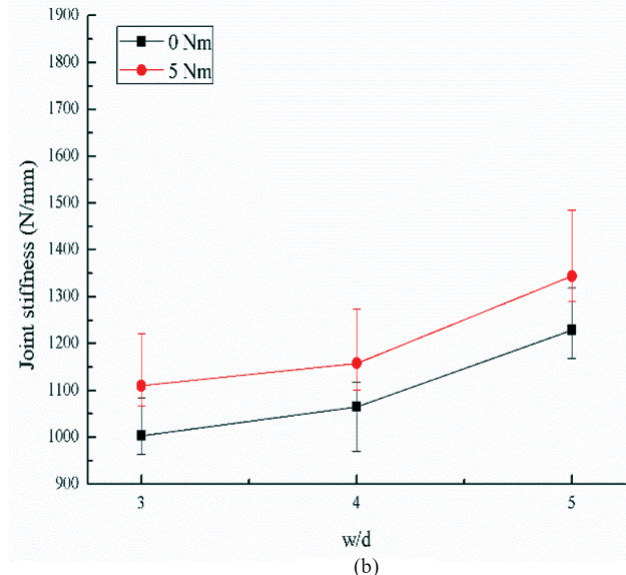
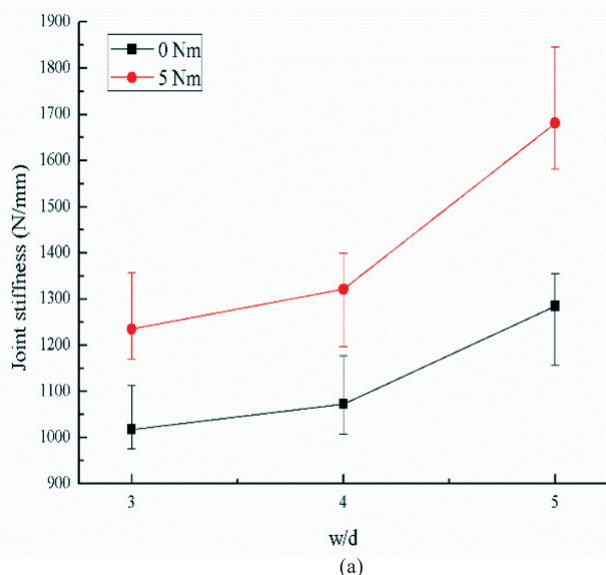


Figure 8. Joint stiffness at  $e/d = 3$  and washer of size (a) 12 mm and (b) 16 mm.

It is observed from Fig. 8 that the slope of the curve with washer diameter 12 mm increases not only with  $w/d$  ratio but also with an increase in the torque. The increase of stiffness with increase in torque was due to the increase in the contact pressure<sup>6</sup>. The trends of the results matches with those given by Khashaba<sup>6</sup>, *et al.* and Rosales-Iriarte<sup>24</sup>, *et al.* Whereas, in case of 16 mm washer diameter, the slope at 5 Nm torque increases with the same slope as it is increasing at a torque of 0 Nm, with respect to  $w/d$  ratio.

For the similar torque conditions, washer with the smaller outer diameter depicts the higher joint stiffness. Under the identical conditions, the pressure applied through the washer of smaller diameter is more and this increases the pressure in the vicinity of hole which may results in the increase in joint stiffness at the initial phase.

**4. NUMERICAL ANALYSIS**

Static structural analysis of single lap single bolt joint was carried out in the ANSYS (Analysis systems) software to find out failure load and failure mode of different joint configurations as shown in Table 2.

In the bolted joint, bolt hole is the region of stress concentration, where the stresses are high, but this high value of stress does not lead to the ultimate failure of joint. Therefore, it becomes difficult to calculate the numerical value of the actual bearing strength of the joint in the presence of the stress concentration around the hole. To address this problem, characteristic curve method<sup>19</sup> is used to predict the failure load and the failure mode of the composite joint around the hole.

Characteristic curve is an artificial curve which is calculated numerically by the compressive and tensile characteristic lengths. The characteristic length may vary with geometry and material, but it is independent of applied load as the stress distribution is not changed, only the magnitude of stresses is changed with respect to the applied load<sup>2</sup>. By using this method, failure of composite joint is determined on characteristic curve instead of edge of bolt hole.

The curve is drawn as per the Eqn. (3) by using the characteristic lengths.

$$r_c = \frac{d}{2} + R_{ot} + (R_{oc} - R_{ot})\cos\theta \tag{3}$$

where  $r_c$  is the radius of characteristic curve,  $R_{ot}$  is the characteristic length in tension and  $R_{oc}$  is the characteristic length in compression.

The characteristic curve is symmetric to the axis of the applied load, and the angle  $\theta$  can be measured either clockwise or anticlockwise from the axis of the applied load. The failure modes are predicted as per Eqn. (4) given by Chang<sup>25</sup>, *et al.*

- $0^\circ \leq \theta \leq 15^\circ$  : Bearing failure
- $30^\circ \leq \theta \leq 60^\circ$  : Shear-out failure
- $75^\circ \leq \theta \leq 90^\circ$  : Net-tension failure

After calculating the characteristic lengths, the characteristic curve was formed around the hole of the model.

Numerically failure load is calculated by Failure Index (*FI*) on the characteristic curve. Tsai-Wu failure criteria<sup>26</sup> shown in Eqn. (5) is used to determine the failure of joint.

$$F_1\sigma_1 + F_2\sigma_2 + F_{11}\sigma_1^2 + F_{22}\sigma_2^2 + F_{66}\sigma_6^2 + 2F_{12}\sigma_1\sigma_2 = FI \tag{5}$$

where  $F_1, F_2, F_{11}, F_{22}, F_{66}$  and  $F_{12}$  are the Tsai-Wu equation polynomial which are associated to the properties of laminate and are calculated experimentally.  $\sigma_1, \sigma_2$  and  $\sigma_6$  are the maximum principle stress, minimum principle stress and maximum shear stress, respectively and are calculated numerically.

The six parameters  $F_1, F_2, F_{11}, F_{22}, F_{66}$  and  $F_{12}$  depend upon longitudinal tensile strength ( $X_t$ ), transverse tensile strength ( $Y_t$ ), longitudinal compressive strength ( $X_c$ ), transverse compressive strength ( $Y_c$ ) and shear failure strength ( $S$ ). Equations (6) to (11) are used to calculate Tsai-Wu polynomials.

$$F_1 = \frac{1}{X_t} - \frac{1}{X_c} \tag{6}$$

$$F_2 = \frac{1}{Y_t} - \frac{1}{Y_c} \tag{7}$$

$$F_{11} = \frac{1}{X_t X_c} \tag{8}$$

$$F_{22} = \frac{1}{Y_t Y_c} \tag{9}$$

$$F_{66} = \frac{1}{S^2} \tag{10}$$

$$F_{12} = -0.5\sqrt{F_{11}F_{22}} \tag{11}$$

In the Eqns. (5) to (11), 1 corresponds to the longitudinal direction of the laminate, 2 corresponds to the transverse direction of the laminate and 6 belongs to the shear component in the 1–2 plane.

$F_{12}$  is the in-plane interaction term, which is expressed in terms of bi-axial strength of the composite.  $F_{11}$  and  $F_1$  are the interactions of longitudinal tensile and compressive strengths.  $F_{22}$  and  $F_2$  are the interactions of transverse tensile and compressive strengths.  $F_{66}$  and  $F_6$  are the interactions of negative and positive pure shear strengths along 1–2 plane.

Failure of the joint can be estimated using Failure Index (*FI*) as given by Eqn. (5). *FI* is a scalar quantity that defines the failure of the joint based upon its following values.

- If  $FI < 1$ , no failure of joint
- If  $FI > 1$ , failure of joint

*FI* was calculated on several points on the characteristic curve and the maximum value of *FI* among these points along with its location on characteristic curve was used to determine the failure mode and failure load of the joint using Eqns. (4) and (12), respectively. The failure load (*F*) of the joint was calculated by Eqn. (12) as the ratio of applied load (*P*) to failure index (*FI*).

Failure load of the joint can be calculated numerically by using the Eqn. (12).

$$F = \frac{P}{FI} \tag{12}$$

where *F* is failure load, *P* is applied load and *FI* is Failure Index at curve. The value of failure index on the characteristic curve defines the mode of failure of joint. For the accuracy

of results, the mesh has been refined around the bolt-hole and along the characteristic curve as shown in Fig. 9. The boundary conditions given to the model are shown in the Fig. 10. One end is fixed with displacements in all directions set to zero. On the other end; the load is applied in two steps. In the first step, bolt pre-tension is applied, and force ( $P$ ) is applied in the second step.

The failure angle on the characteristic curve, for a typical joint configuration with  $w/d = 5$ ,  $e/d = 3$ , and 5 Nm torque on the washer of outer diameter 12 mm is as shown in Fig. 11 which demonstrated the bearing failure mode. The failure load and failure mode for each geometric configuration are shown in Table 3, where,  $B$  stands for bearing, and  $NT$  is the net-tension mode of failure. It can be seen from Table 3 that there is a good agreement between the experimental and numerical results.

## 5. CONCLUSIONS

From the experimental as well as the numerical results of single lap single bolt joint, the following conclusions can be drawn.

- (i) Failure load and the stiffness of the single lap bolt joint has shown a direct relation to the width-to-diameter ratio ( $w/d$ ). Increasing  $w/d$  ratio, failure load, and stiffness are increased. Failure load increases up to the critical value of the  $w/d$  ratio *i.e.*,  $w/d = 4$  for 0 Nm, and  $w/d = 5$  for 5 Nm torque.
- (ii) Bolt torque/preload has shown a significant effect on the failure load and the failure mode of the bolt joint. Although for similar  $e/d$  ratios and washer configurations, at a low

**Table 3. Comparison of failure load and failure mode of experimental and numerical results**

Specimen	Failure load (N)		Failure Mode	
	Experimental	Numerical	Experimental	Numerical
1	3640	3235	NT	NT
2	4550	3868	NT	NT
3	4730	4021	NT	NT
4	5410	4760	NT	NT
5	5910	5378	NT	NT
6	4020	3819	B	B
7	5810	5345	B	NT
8	5865	5161	B	NT
9	7040	6124	B+NT	NT
10	7955	7005	B+NT	NT
11	4080	3916	B	B
12	6380	5805	B	B
13	6505	6049	B	B
14	8260	7351	B	B
15	9250	8047	B	B
16	3810	3581	B+NT	NT
17	4590	4131	NT	NT
18	4780	4398	NT	NT
19	5460	4914	NT	NT
20	5950	5415	NT	NT
21	3980	3781	B	B
22	6050	5566	B	B
23	6155	5601	B	B
24	7230	6362	B+NT	NT
25	8165	7186	B+NT	NT
26	4110	3945	B	B
27	6420	5778	B	B
28	6560	5904	B	B
29	8310	7396	B	B
30	9180	8170	B	B

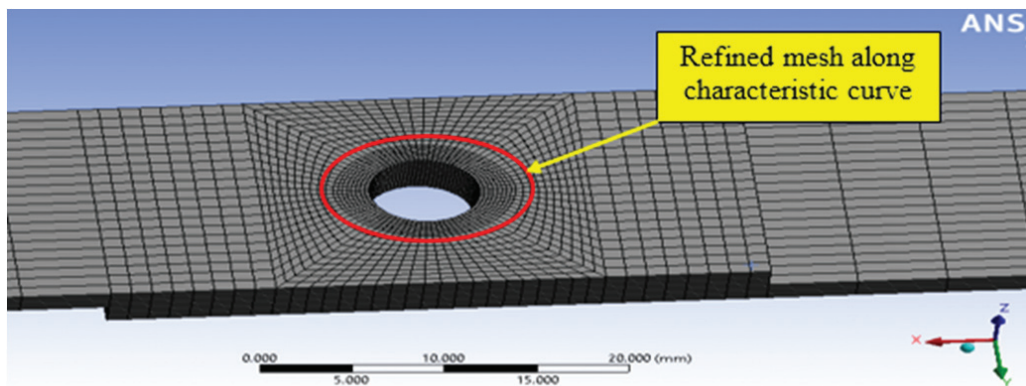


**Figure 9. Mesh around the hole.**

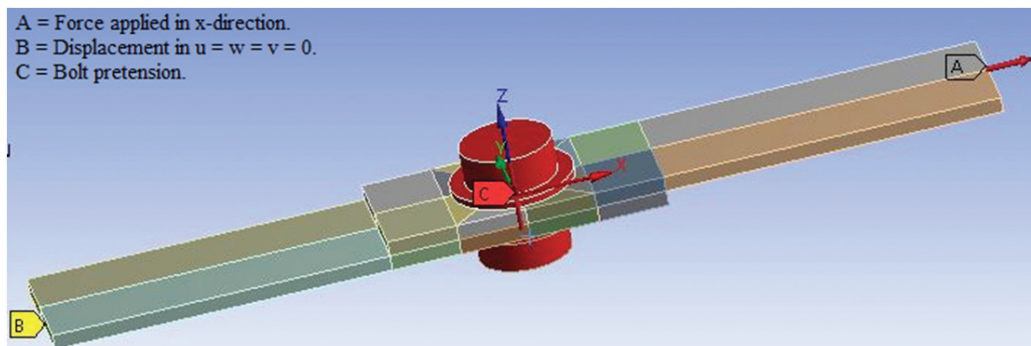


**Figure 10. Boundary conditions given to the specimen.**

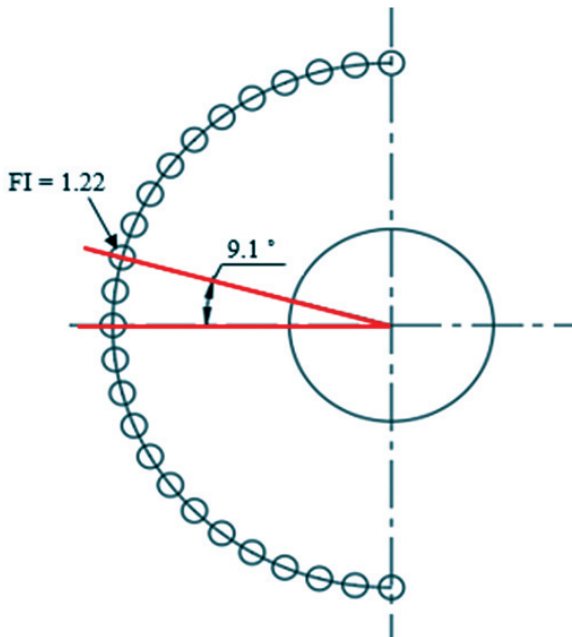


**Figure 11. Measurement of failure mode and load on the characteristic curve.**

value of  $w/d$  ratio, failure load increased when preload was increased from 0 Nm to 5 Nm, the failure became catastrophic. Whereas, beyond the critical value of  $w/d$  ratios, at which bearing mode of failure develops, failure became non-catastrophic for both torque levels. However, there was a significant difference between their failure loads.

- (iii) The failure mode of a single lap bolt joint changes from net-tension to bearing with an increase in  $w/d$  ratio. However, the critical value of  $w/d$  ratio is different for the joints tightened at different torque levels.
- (iv) The stiffness of the bolt joint depends upon the bolt preload and outer diameter of the washer. The joint stiffness increases with increase in the bolt preload, whereas an increase in the outer diameter of washer has a negative effect on the joint stiffness.
- (v) For the specimen with a particular  $w/d$  ratio, bolt preload, and outer diameter of the washer, no change in joint performance, *i.e.* the ultimate load-bearing capacity and the stiffness of joint, was observed by increasing the  $e/d$  ratio  $> 3$ .
- (vi) Numerical analysis of the bolt joint using characteristic curve method along with Tsai-Wu failure theory gave a good correlation with the experimental results.

## REFERENCES

1. McCarthy, M.; Lawlor, V.P.; Stanley, W.F. & McCarthy, C.T. Bolt-hole clearance effects and strength criteria in single-bolt, single-lap, composite bolted joints. *Compos. Sci. Technol.*, 2002, **62**(11), 1415-1431. doi: 10.1016/S0266-3538(02)00088-X
2. Kweon, J.H.; Ahn, H.S. & Choi, J.H. A new method to determine the characteristic lengths of composite joints without testing. *Compos. Struct.*, 2004, **66**(2), 305-315. doi: 10.1016/j.compstruct.2004.04.053
3. Xiao, Y. & Ishikawa, T. Bearing strength and failure behavior of bolted composite joints (part I: Experimental investigation). *Compos. Sci. Technol.*, 2005, **65**(7), 1022-1031. doi: 10.1016/j.compscitech.2005.02.011
4. Xiao, Y. & Ishikawa, T. Bearing strength and failure behavior of bolted composite joints (part II: modeling and simulation). *Compos. Sci. Technol.*, 2005, **65**(7), 1032-1043. doi: 10.1016/j.compscitech.2004.12.049
5. Kelly, G. Quasi-static strength and fatigue life of hybrid (bonded/bolted) composite single-lap joints. *Compos. Struct.*, 2006, **72**(1), 119-129. doi: 10.1016/j.compstruct.2004.11.002
6. Khashaba, U.; Sallam, H.E.M.; Al-Shorbagy, A.E. & Seif, M.A. Effect of washer size and tightening torque on the performance of bolted joints in composite structures. *Compos. Struct.*, 2006, **73**(3), 310-317. doi: 10.1016/j.compstruct.2005.02.004
7. Nassar, S.A.; Virupaksha, V.L. & Ganeshmurthy, S. Effect of bolt tightness on the behavior of composite joints. *J. Press. Vess. T.*, 2007, **129**(1), 43-51. doi: 10.1115/1.2389000
8. Sen, F.; Pakdil, M.; Sayman, O. & Benli, S. Experimental failure analysis of mechanically fastened joints with clearance in composite laminates under preload. *Mater. Design*, 2008, **29**(6), 1159-1169. doi: 10.1016/j.matdes.2007.05.009
9. Asi, O. Effect of different woven linear densities on the bearing strength behaviour of glass fibre reinforced epoxy composites pinned joints. *Compos. Struct.*, 2009, **90**(1), 43-52. doi:10.1016/j.compstruct.2009.01.007
10. Egan, B.; McCarthy, C.T.; McCarthy, M.A. & Frizzell, R.M. Stress analysis of single-bolt, single-lap, countersunk composite joints with variable bolt-hole clearance. *Compos. Struct.*, 2012, **94**(3), 1038-1051. doi: 10.1016/j.compstruct.2011.10.004
11. Irisarri, F.X.; Laurin, F.; Carrere, N. & Maire, J.F. Progressive damage and failure of mechanically fastened joints in CFRP laminates—Part I: Refined Finite Element modelling of single-fastener joints. *Compos. Struct.*, 2012, **94**(8), 2269-2277. doi: 10.1016/j.compstruct.2011.07.023
12. Qin, T.; Zhao, L. & Zhang, J. Fastener effects on mechanical behaviors of double-lap composite joints. *Compos. Struct.*, 2013, **100**(1), 413-423. doi: 10.1016/j.compstruct.2013.01.008
13. Gray, P.; O'Higgins, R. & McCarthy, C. Effects of laminate thickness, tapering and missing fasteners on the mechanical behaviour of single-lap, multi-bolt, countersunk composite joints. *Compos. Struct.*, 2014, **107**(1), 219-230. doi: 10.1016/j.compstruct.2013.07.017
14. Zhai, Y.; Li, D.; Li, X.; Wang, L. & Yin, Y. An experimental study on the effect of bolt-hole clearance and bolt torque on single-lap, countersunk composite joints. *Compos.*

- Struct.*, 2015, **127**(1), 411-419.  
doi: 10.1016/j.compstruct.2015.03.028
15. Sekhon, M.; Saini, J.S.; Singla, G. & Bhunia, H. Influence of nanoparticle fillers content on the bearing strength behavior of glass fibre-reinforced epoxy composites pin joints. *P. I. Mech. Eng. L-J. Mat.*, 2017, **231**(8), 641-656. doi: 10.1177/1464420715607556
  16. Singh, S.; Saini, J.S. & Bhunia, H. Investigation on failure modes for pin joints made from unidirectional glass-epoxy nanoclay laminates. *Fatigue Fract. Eng. M.*, 2016, **39**(3), 320-334. doi: 10.1111/ffe.12358
  17. Mara, V.; Haghani, R. & Al-Emrani, M. Improving the performance of bolted joints in composite structures using metal inserts. *J. Compos. Mater.*, 2016, **50**(21), 3001-3018. doi: 10.1177/0021998315615204
  18. Singh, K.; Saini, J.S. & Bhunia, H. Effect of Metallic Inserts on the Strength of Pin Joints Prepared from Glass Fibre Reinforced Composites, *Def. Sci. J.*, 2017, **67**(5), 592-600. doi : 10.14429/dsj.67.11041
  19. Chani, K.S.; Saini, J.S. & Bhunia, H. Effect of nanoclay and bolt preloads on the strength of bolted joints in glass epoxy nanocomposites. *J. Braz. Soc. Mech. Sci.*, 2018, **40**(4), 184 (1-19). doi: 10.1007/s40430-018-1108-6
  20. ASTM D3039 / D3039M-17, Standard Test Method for Tensile Properties of Polymer Matrix Composite Materials, ASTM International, West Conshohocken, PA, 2017, www.astm.org. (Accessed on 03 July 2017). doi: 10.1520/D3039\_D3039M-17
  21. ASTM D695-15, Standard Test Method for Compressive Properties of Rigid Plastics, ASTM International, West Conshohocken, PA, 2015, www.astm.org. (Accessed on 03 July 2017). doi:10.1520/D0695-15
  22. ASTM D5379 / D5379M-12. Standard test method for shear properties of composite materials by the V-notched beam method. ASTM International, West Conshohocken, PA, 2012, www.astm.org. (Accessed on 03 July 2017). doi:10.1520/D5379\_D5379M-12
  23. Park, H.J. Effects of stacking sequence and clamping force on the bearing strengths of mechanically fastened joints in composite laminates. *Compos. Struct.*, 2001, **53**(2), 213-221. doi: 10.1016/S0263-8223(01)00005-8
  24. Rosales-Iriarte, F.; Fellows, N. & Durodola, J. Experimental evaluation of the effect of clamping force and hole clearance on carbon composites subjected to bearing versus bypass loading, *Compos. Struct.*, 2011, **93**(3), 1096-1102. doi:10.1016/j.compstruct.2010.09.016
  25. Chang, F.K.; Scott, R.A. & Springer, G.S. Strength of mechanically fastened composite joints. *J. Compos. Mater.*, 1982, **16**(6), 470-494. doi: 10.1177/002199838201600603
  26. Tsai, S.W. & Wu, E.M. A general theory of strength for anisotropic materials. *J. Compos. Mater.* 1971, **5**(1), 58-80. doi: 10.1177/002199837100500106

## CONTRIBUTORS

**Mr Jaspreet Singh** received his ME (Computer Aided Design and Manufacturing Engineering) from Thapar Institute of Engineering and Technology, Patiala, Punjab. His research work involves analysis of mechanical joints prepared from polymer materials.

In the current study, he is involved in literature review, preparation of laminates, preparation and experimental testing of the mechanical joints.

**Mr Kulwinder Singh** is pursuing his doctoral from Thapar Institute of Engineering and Technology, Patiala, Punjab. His research work involves analysis of mechanical joints prepared from polymer nanocomposite materials.

In the current study, he is involved in experimental testing of mechanical joints and their analysis using finite element methods.

**Dr J.S. Saini** is working as Associate Professor in Mechanical Engineering Department at Thapar Institute of Engineering and Technology, Patiala, Punjab. His specialisation is design and analysis. He has nearly 30 research papers in various journals and conferences. Presently he is working in the area of nano composites and their analysis.

In the current study, he is involved in literature review, material selection, purchasing of material, preparation of glass fibre reinforced laminates and analysis of the results.